

# We are IntechOpen, the world's leading publisher of Open Access books Built by scientists, for scientists

6,900

Open access books available

186,000

International authors and editors

200M

Downloads

Our authors are among the

154

Countries delivered to

TOP 1%

most cited scientists

12.2%

Contributors from top 500 universities



WEB OF SCIENCE™

Selection of our books indexed in the Book Citation Index  
in Web of Science™ Core Collection (BKCI)

Interested in publishing with us?  
Contact [book.department@intechopen.com](mailto:book.department@intechopen.com)

Numbers displayed above are based on latest data collected.  
For more information visit [www.intechopen.com](http://www.intechopen.com)



# Circuit Models of Bioelectric Impedance

*Alexandru Gabriel Gheorghe, Florin Constantinescu,  
Miruna Nițescu and Mihai Eugen Marin*

## Abstract

Accurate information about fluid distribution in different compartments of the human body is very important in various areas of medicine like drug dosage, renal replacement therapy, nutritional support, coronary artery disease, colorectal cancer and HIV infection. The body impedance analysis method being simple, inexpensive, accurate and noninvasive is largely used to this end. Several models of the body impedance are presented in this chapter. The first is the Cole model, a linear, first-order  $RC$  circuit valid for a frequency range of two decades. Another model, developed by De Lorenzo, employs a fractional-order impedance whose parameters are identified using the frequency characteristics of the impedance module and can be used for a frequency range of three decades. In addition, two other models are presented, a ladder  $RC$  model valid for a frequency range of two decades and its extension to three decades, as well as a circuit containing multiple  $RC$  branches connected in parallel. These two models are obtained by approximating the measured body admittance modulus with a physically realizable circuit function followed by the circuit synthesis. The last model can be simplified, its simplest form being the Cole model. Allowing a better prediction of the intracellular and extracellular water volumes, this model can be viewed as an extension of the Cole model.

**Keywords:** bioimpedance, circuit synthesis, frequency response, impedance measurement, passive circuits

## 1. Overview

In various areas of medicine like drug dosage, renal replacement therapy and nutritional support, an accurate information about fluid distribution in different compartments of the body may lead to significant conclusions. Dilution methods, magnetic resonance imaging, computer axial tomography and X-ray method used to determine the fat-free mass are expensive, time consuming and unfit for routine procedures, demanding laboratories and highly trained technicians. The body impedance analysis method being simple, inexpensive, accurate and noninvasive has become largely used to predict the fluid distribution in different compartments of the body: intracellular water (ICW), extracellular water (ECW) and total body water (TBW) [1–6]. Several variants of the body impedance analysis method have been reported: single-frequency and dual-frequency bioimpedance analysis (BIA) and multi-frequency bioimpedance analysis which is also called bioimpedance spectroscopy (BIS).

Intracellular water (ICW) can be used to estimate body cell mass (BCM) which is an important indicator of the nutrition status. The evaluation of extracellular water (ECW) is also important to predict changes in fluid distribution for people suffering from wasting diseases, obesity, or patients receiving dialysis [6].

Section 2 describes the well-known Cole model, a linear, first-order RC circuit of the human body used for ICW and ECW volume prediction. Section 3 presents a fractional-order impedance whose parameters are identified using the frequency characteristics of the impedance module and can be used for a frequency range of up to three decades. In Section 4, two versions of a ladder RC model are presented, one valid for a frequency range of two decades and its extension valid for three decades. Section 5 describes a model consisting of multiple RC branches connected in parallel. This model can be viewed as an extension of the Cole model. Finally, some conclusions are presented in Section 6.

## 2. Cole model

### 2.1 Introduction

The frequency dependence of the body impedance, measured for example between the wrist and the ankle, can be understood knowing the behavior of the organic tissue at low frequencies (LF) and at high frequencies (HF). In the LF range (1–70 kHz), the cell membrane capacity has a high impedance value and the electric current flows mainly through ECW (**Figure 1a**). In the HF range (70 kHz–1 MHz), as this impedance decreases, the current flows through both ICW and ECW depending on their relative conductivities and volumes [7] (**Figure 1b**).

At a first glance, this behavior can be modeled with a very simple linear electrical circuit known as the Cole model [2–4] which is shown in **Figure 2**, where:

- $R_i$  stands for the resistance of the intracellular fluid;
- $C_m$  is the capacity of the cellular membrane; and
- $R_e$  stands for the resistance of the extracellular fluid.

The AC equivalent resistance of this circuit at zero frequency is  $R_0 = R_e$  and its AC equivalent resistance at infinite frequency is  $R_\infty = (R_i \cdot R_e)/(R_i + R_e)$ .

Approximating  $R_0$  with the measured AC resistance at the minimum angular frequency  $\omega_m$  and  $R_\infty$  with the measured AC resistance at the maximum angular frequency  $\omega_M$ , the ICW volume  $V_I$  and the ECW volume  $V_E$  are estimated [3] as:

$$V_I = k_I \cdot Wt \cdot (Ht^2/R_i) \quad (1)$$

$$V_E = k_E \cdot Wt \cdot (Ht^2/R_e) \quad (2)$$

where  $Ht$  is the height,  $Wt$  is the weight of the subject and  $k_I$  and  $k_E$  are constants that can be determined by the cross validation against other methods [2–3].

### 2.2 Analysis of measurement results

Some measurement results for a bioimpedance have been reported in [4] together with a circuit model of the test bench (**Figure 3**). This circuit that includes the Cole model can be used for simulation purposes. In order to estimate the effect

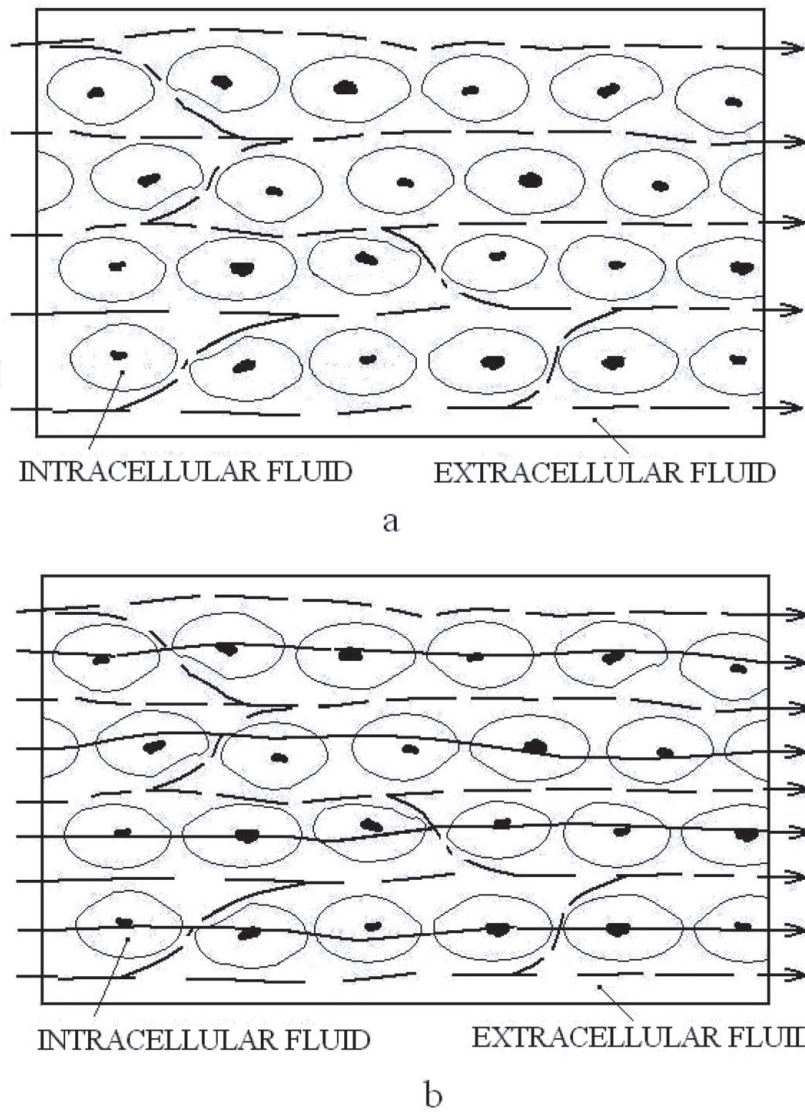


**Figure 1.**  
The organic tissue behavior for: (a) LF electrical current flow and (b) HF electrical current flow [7].

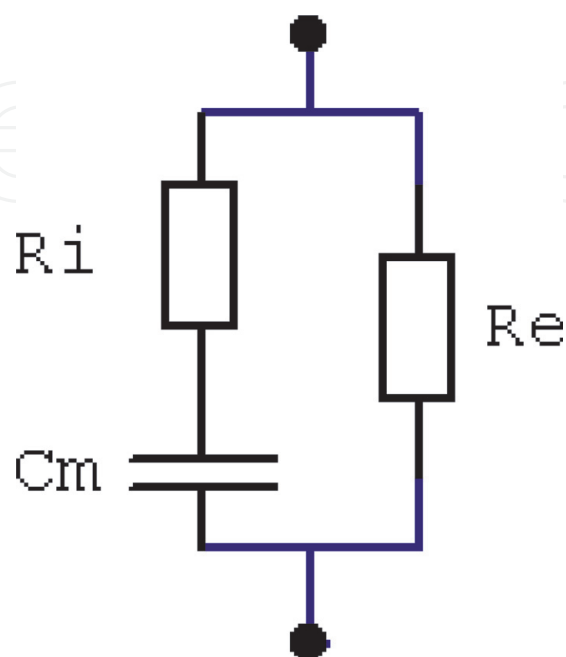


**Figure 2.**  
Cole model.

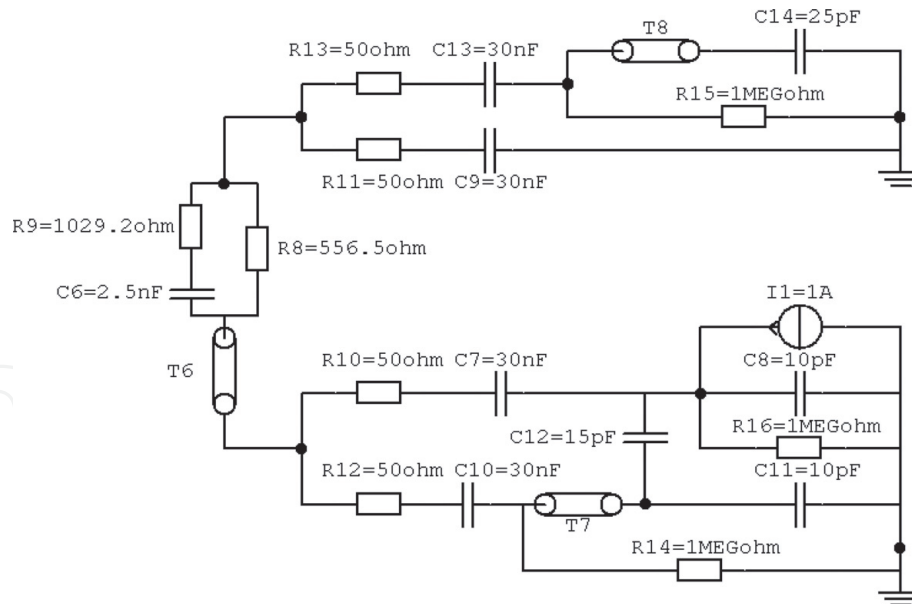


**Figure 3.** The Cole model and the equivalent circuit of the measurement equipment (Model 1).

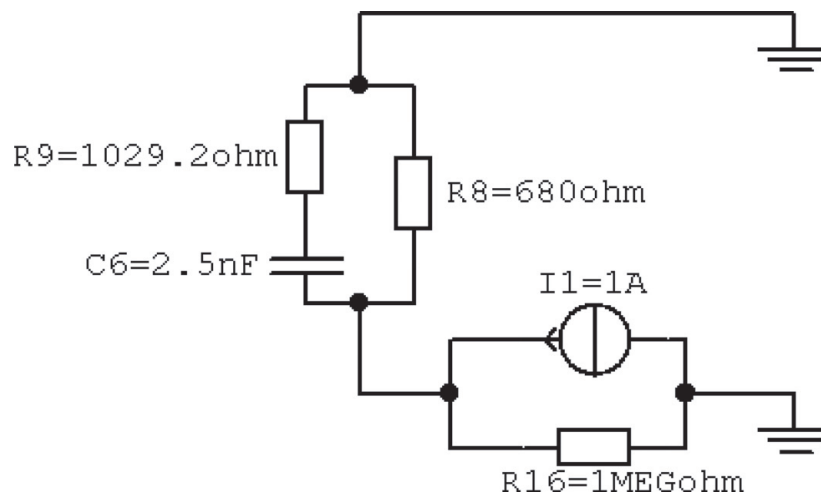


**Figure 4.** The Cole model and the simplified circuit (Model 2).

of the measurement equipment (signal source, cables and connectors), the circuit in **Figure 3** has been simulated. Similar results are obtained by simulating a simpler circuit made only of the Cole model and the signal source (**Figure 4**). The frequency characteristics of the circuit which takes into account the measurement equipment (Model 1) and of the Cole model only (Model 2) are given in **Figure 5**. It follows that the measurement equipment has practically no influence and the result of the measurements is exactly the frequency characteristic of the human body bioimpedance [8].

The measured values of the human body impedance as a function of frequency are given in **Table 1** [3].

### 2.3 Parameter identification

The parameters of the Cole model with the frequency independent values for  $R_b$ ,  $C_m$  and  $R_e$  can be identified using the measured impedance values for three

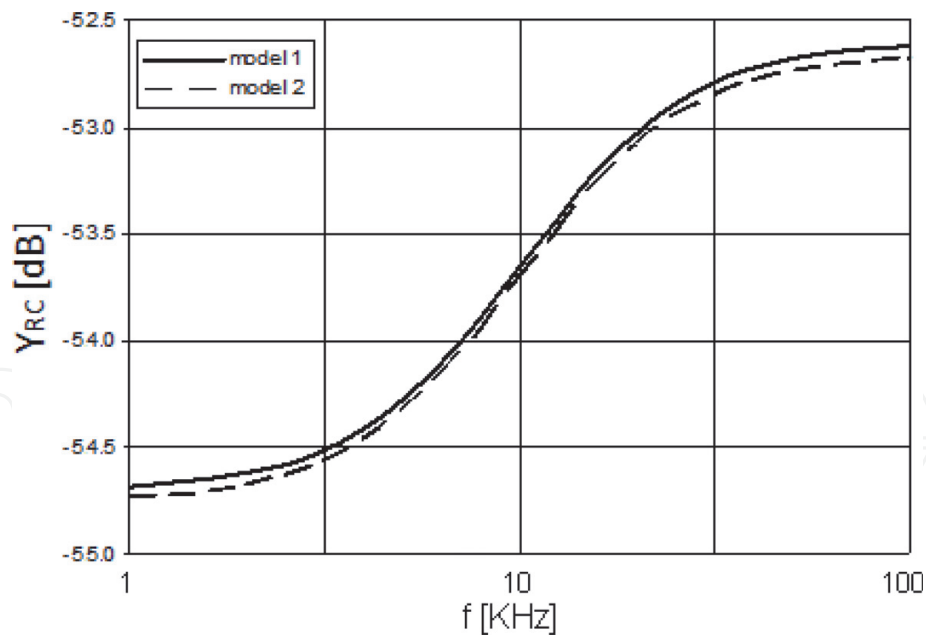


**Figure 5.**  
 Simulation results for Model 1 and Model 2.

Frequency [kHz]	Measured impedance [ohm]
1.00E+03	5.62E+02
2.00E+03	5.58E+02
3.00E+03	5.54E+02
4.00E+03	5.50E+02
5.00E+03	5.46E+02
1.00E+04	5.29E+02
1.50E+04	5.13E+02
2.00E+04	5.00E+02
2.50E+04	4.88E+02
5.00E+04	4.52E+02
7.50E+04	4.30E+02
1.00E+05	4.18E+02
1.28E+05	4.08E+02
1.48E+05	4.02E+02
1.60E+05	4.00E+02
2.00E+05	3.92E+02
2.48E+05	3.85E+02
5.00E+05	3.66E+02
7.48E+05	3.58E+02
1.00E+06	3.53E+02

**Table 1.**  
 The measured human body impedance.

frequencies. As the resistance values at the minimum and maximum frequencies are used for ECW and ICW volume estimation in Eqs. (1) and (2), we have chosen these three frequencies as  $\omega_1 = \omega_m$ ,  $\omega_2 = \omega_M$ , and  $\omega_3$  corresponding to the intersection points between the measured characteristic and that of the Cole model (Figure 6). In this case, it is obvious that the results obtained with this Cole model are not fitted to the measured data. This proves that a more accurate model is necessary. Identifying the parameters of this Cole model in a different way, that is, using three frequencies in the middle of the frequency interval, significant errors appear at the minimum and maximum frequencies. It follows that the Cole model is not suitable for ECW and ICW computation [8].

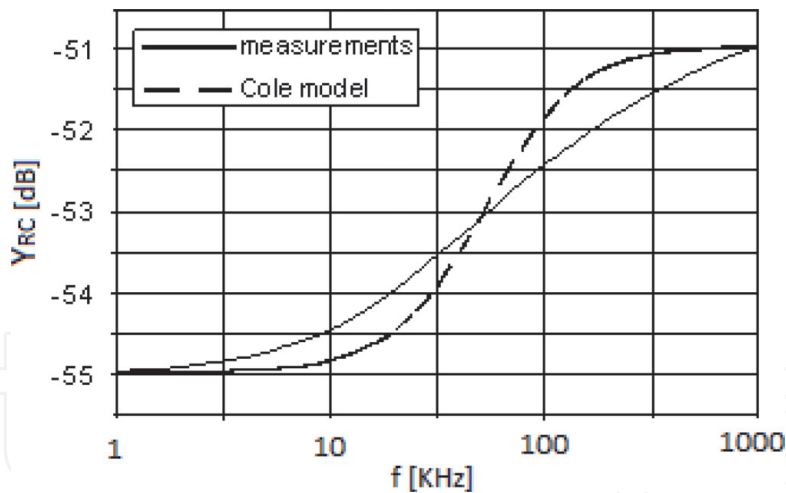


**Figure 6.**  
The simulated Cole model and the measured results.

### 3. De Lorenzo model

The measurement results show that, in a wide frequency range (e.g., for two or three decades), the parameters of the circuit are frequency dependent and the relationships between the resistances of this model and the body water volumes are nonlinear. For example:

- the electrical permittivity depends on frequency as it is pointed out in **Figure 7** [3];
- the mixture effects have a greater influence on the skeletal muscle resistivity in the LF range than in the HF range [3]; and
- due to the complexity of the nonlinear relations between  $R_i$  and  $R_e$  and ICW and ECW volumes, some heuristic relations as Eqs. (1) and Eq. (2), including the height and weight of the subject are used to compute the body water volumes.

The above properties, including unusual high values of the dielectric constant are discussed in detail in [3, 9]. As our approach is not related to these aspects, we suggest the interested researchers to read these publications.

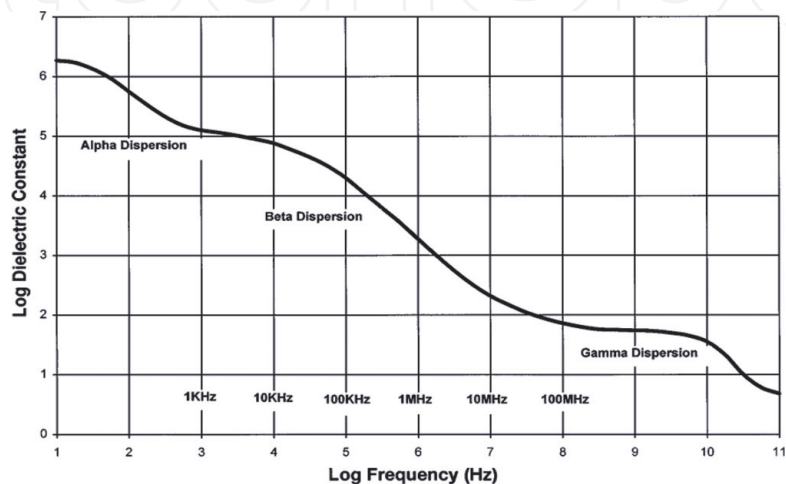


**Figure 7.**  
Dielectric constant of the muscle tissue vs. frequency [3].

Over 500 kHz, the time delay between the excitation and its response cannot be neglected [3]. In this case, a model with distributed parameters could be more accurate.

As it was shown in the previous section, the frequency characteristic of the Cole model with frequency independent values  $R_i$ ,  $C_m$  and  $R_e$  cannot be fitted to the measured data on a three-decade frequency range. In order to fix this drawback, a modified Cole model has been proposed in [3] in which the body impedance is considered as:

$$Z_{RC}(j\omega) = \left( \frac{R_e}{R_e + R_i} \right) \left( R_i + \frac{R_e}{1 + [j\omega C_m (R_e + R_i)]^\alpha} \right) e^{-j\omega T_d} \quad (3)$$

where  $\omega$  is the angular frequency,  $T_d$  is the delay and  $\alpha \in [0.3, 0.7]$  is a coefficient whose value is chosen to fit the values given by Eq. (3) to the  $|Z_{RC}(j\omega)|$  experimental data. As this formula does not lead to a single valued function  $\arg(Z_{RC}(j\omega))$ , the identification of its parameters based on the measured frequency characteristics  $|Z_{RC}(j\omega)|$  and  $\arg(Z_{RC}(j\omega))$  cannot be made. The measurements of  $|Z_{RC}(j\omega)|$  and  $\arg(Z_{RC}(j\omega))$  suggest a circuit like that in **Figure 2** having frequency dependent components, rather than this formula that has been obtained starting from the equivalent impedance of the linear circuit in **Figure 2** in which the power  $\alpha < 1$  is attached to one term while other terms remain unchanged. Taking into account that the frequency dependence of material parameters is not known for all kinds of tissues, the development of an accurate physical model is very difficult or even impossible [10].

The parameter identification for Eq. (3) is made in [3] (ignoring the uncertainty on phase) starting from measured frequency characteristics  $|Z_{RC}(j\omega)|$ . A very good fitting of the model characteristics to the experimental data is obtained in this case which describes de Lorenzo model. But the real parts of the body impedance in Eq. (3) at  $\omega_m$  and  $\omega_M$  have not the dimension of AC resistances, so the formulae Eq. (1) and Eq. (2) aimed to be employed with the Cole model AC resistances cannot be used properly.

## 4. RC ladder model

### 4.1 Introduction

The parameters of a model with a given structure are extracted or identified using optimization methods. In general, these methods minimize the distance between the measurement results and those obtained by simulation. In the case of semiconductor devices, the parameters of the large signal DC models or those of the small signal AC models are usually extracted using numerical techniques. Some symbolic methods have been used efficiently for parameter identification [11–13]. The circuit functions are generated using a symbolic method, obtaining analytical formulae in terms of  $s$  and model parameters. These parameters are computed using an optimization method to reach a global minimum of the distance between the measured and simulated values of the circuit functions for a set of test frequencies. The symbolic methods are very efficient for the computation of derivatives which are usually needed in the optimization procedure. The optimization can be performed using genetic algorithms [14]. Sometimes, hierarchical techniques are employed to obtain combined DC-AC models [15].

The body impedance analysis method has not yet reached its full potential. Following the trend to improve the method by increasing the level of model accuracy, a new approach to the parameter identification for a linear RC model in

bioimpedance spectroscopy is presented in this section. This approach employs the approximation of the measured body admittance modulus  $|Y_{RC}(j\omega)|$  with a physically realizable function followed by the circuit synthesis [16]. This model is a linear RC circuit with frequency independent values of resistances and capacitances. As the frequency dependence of the phase angle  $\arg(Y_{RC}(j\omega))$  can be computed from  $|Y_{RC}(j\omega)|$  using the Bayard-Bode relationships [17], the measured values of  $\arg(Y_{RC}(j\omega))$  are not needed for the parameter identification of this model. Two equivalent circuits of the human body, built using this approach, have been proposed [10–11]. These are ladder circuits which cannot be considered as extensions of the Cole model.

## 4.2 RC admittance synthesis

The synthesis method for an RC admittance ( $Y_{RC}$ ) developed in [15] can be used also for an RC impedance ( $Z_{RC} = 1/Y_{RC}$ ) with some minor modifications, and it is presented in the following.

A function  $F(s)$  of a complex variable  $s$  is an RC admittance if and only if the following conditions are fulfilled:

- $F(s)$  is a rational fraction of  $s$  with real coefficients;
- the poles and zeros of  $F(s)$  are simple and alternate on the negative real axis, the closest to the origin being a zero; and
- the number of zeros of  $F(s)$  is equal or greater with one with respect to the number of poles  $F(s)$ .

Replacing  $s$  with  $j\omega$ , (where  $\omega=2\pi f$  and  $f$  is the frequency) the shape of the RC admittance modulus curve  $|Y_{RC}(j\omega)|$  versus  $\omega$  is defined by the poles and zeros location. Sweeping the  $\omega$  axis starting from the origin, it can be observed that the location of a zero is associated with a slope change of 20 dB/decade and the location of a pole is associated with a slope change of  $-20$  dB/decade. This is because the characteristic  $|Y_{RC}(j\omega)|$  has asymptotes whose slopes are 20 dB/decade, 0, 20 dB/decade, 0, and so on. The  $|Y_{RC}(j\omega)|$  characteristic approximation by asymptotes has the maximum error of 3 dB at the asymptote intersection (Figure 8) [16].

A natural way to approximate the  $|Y_{RC}(j\omega)|$  characteristic is to consider a smaller asymptote number than that corresponding to the measured characteristic. A greater error  $\varepsilon$  between measured and simulated values leads to a simpler circuit (Figure 8).

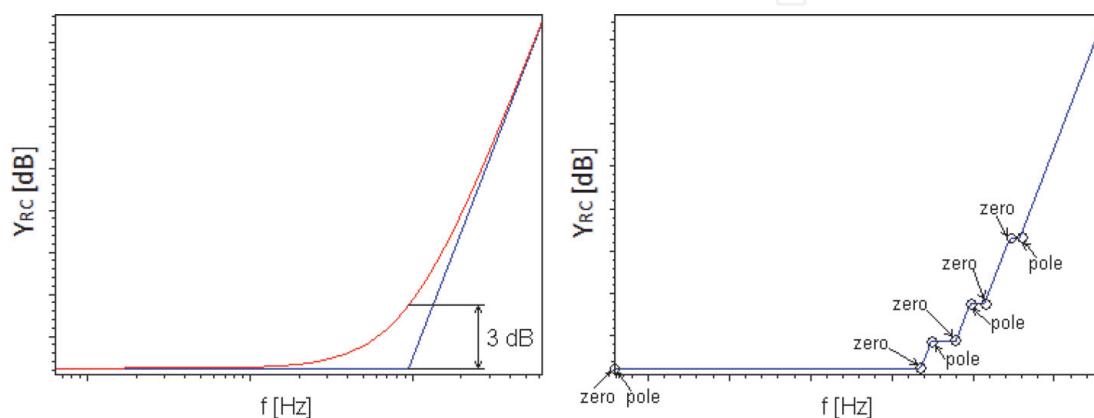


**Figure 8.**  
The  $|Y_{RC}(j\omega)|$  characteristic approximation by asymptotes.

The algorithm for the synthesis of a  $RC$  one-port in the angular frequency band  $[\omega_m, \omega_M]$ , where  $\omega_m$  is the minimum value and  $\omega_M$  is the maximum value, has the following steps [16]:

- set the first zero  $z_1$  corresponding to the minimum angular frequency  $\omega_m$ ;
- compute the remaining poles and zeros at slope changes, by sweeping the  $\omega$  axis with the step  $\Delta\omega$ ; a larger  $\Delta\omega$  leads to a simpler circuit;
- compute the  $RC$  admittance expression; and
- compute the circuit parameters using a synthesis method.

Sweeping the frequency axis with a step  $\Delta\omega_m$ , the algorithm checks the error between the 20 dB/decade asymptote and the given characteristic. This error cannot be greater than an imposed value  $\varepsilon$ . The first pole  $p_1$  is assigned to the last value before that corresponding to an error of  $2\varepsilon$  or greater. If this error occurs after the first angular frequency step  $\Delta\omega_m$ , then  $p_1$  is placed in the vicinity of  $z_1$ . Afterwards, the first asymptote is translated so that a maximum error of  $\varepsilon$  is obtained. The other asymptotes are determined similarly, in order to fulfill the condition  $error \leq \varepsilon$  for each asymptote.

### 4.3 Parameter identification for the two-decade model

The following models are build starting from measurement of the body impedance frequency characteristic  $|Z_{RC}(j\omega)|$  reported in [3, 8]. The simulations presented in Section 2 show that the result of the frequency characteristic measurement is an accurate representation of the human body impedance modulus. Using the above algorithm it follows:

$$Y_{RC}(s) = \frac{17.81 \cdot 10^{-4} (15.92 \cdot 10^{-5}s + 1) (10.23 \cdot 10^{-6}s + 1) (26.82 \cdot 10^{-7}s + 1) (28.82 \cdot 10^{-8}s + 1)}{(15.91 \cdot 10^{-5}s + 1) (86.25 \cdot 10^{-7}s + 1) (22.70 \cdot 10^{-7}s + 1)} \quad (4)$$

Using a Cauer synthesis, the continued fraction expansion in Eq. (5) is obtained, and the circuit is given in **Figure 9**. The parameter values extracted from Eq. (5) are given below.

$$Y_{RC}(s) = 71.97 \cdot 10^{-11}s + \frac{1}{410.65 + \frac{1}{31.08 \cdot 10^{-9}s + \frac{1}{106.17 + \frac{1}{18.16 \cdot 10^{-8}s + \frac{1}{44.66 + \frac{1}{15.69 \cdot 10^{-3}s + 98.64}}}}}}}} \quad (5)$$

A comparison between the frequency characteristic of the  $RC$  ladder model, the Cole model and the measured results is given in **Figure 10**.

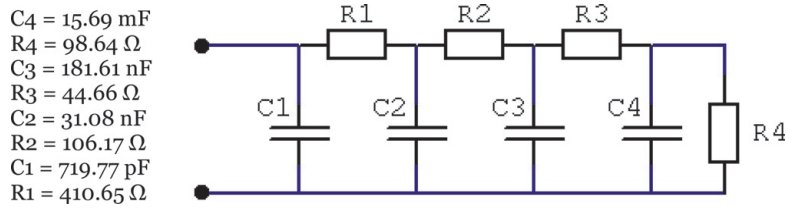


**Figure 9.**  
Cauer synthesis of the RC ladder circuit model [8].

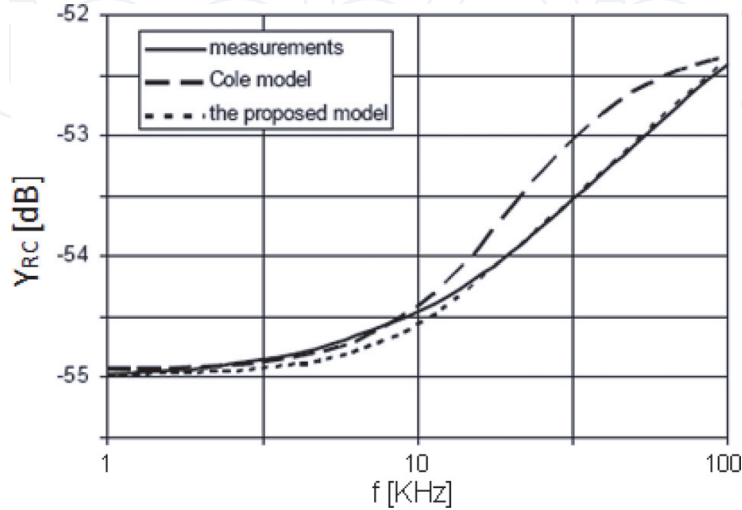


**Figure 10.**  
The frequency characteristic for the Cole model, the two-decade RC ladder model and the measured results.

#### 4.4 Parameter identification for the three-decade model

Using the same algorithm presented above applied for the measurement set of three decades, a more elaborated admittance expression, given in Eq. (6), is obtained [18]. The Cauer synthesis starting from the continued fraction expansion in Eq. (7) gives the circuit presented in **Figure 11**. The parameter values are given above the model. A comparison between the frequency characteristic of the new model and the measured results is given in **Figure 12**.

$$Y_{RC}(s) = \frac{17.81 \cdot 10^{-4} (15.92 \cdot 10^{-5}s + 1)(13.04 \cdot 10^{-6}s + 1)(43.11 \cdot 10^{-7}s + 1)(18.59 \cdot 10^{-7}s + 1)(75.82 \cdot 10^{-9}s + 1)}{(15.91 \cdot 10^{-5}s + 1)(11.55 \cdot 10^{-6}s + 1)(38.08 \cdot 10^{-7}s + 1)(16.47 \cdot 10^{-7}s + 1)} \quad (6)$$

$$Y_{RC}(s) = \frac{1}{19.47 \cdot 10^{-11}s + \frac{1}{392.53 + \frac{1}{23.94 \cdot 10^{-9}s + \frac{1}{109.02 + \frac{1}{10.71 \cdot 10^{-8}s + \frac{1}{42.54 + \frac{1}{50.07 \cdot 10^{-8}s + \frac{1}{17.39 + \frac{1}{16.95 \cdot 10^{-3}s + 106.8}}}}}}}}}}}} \quad (7)$$

$C_5 = 16.99 \text{ mF}$ ,  $R_5 = 106.80 \text{ } \Omega$ ,  $C_4 = 500.71 \text{ nF}$ ,  $R_4 = 17.39 \text{ } \Omega$ ,  $C_3 = 107.12 \text{ nF}$ ,  
 $R_3 = 42.54 \text{ } \Omega$ ,  $C_2 = 23.94 \text{ nF}$ ,  $R_2 = 109.02 \text{ } \Omega$ ,  $C_1 = 194.77 \text{ pF}$ ,  $R_1 = 392.53 \text{ } \Omega$ .

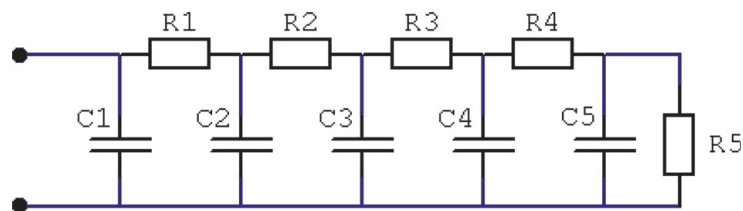


**Figure 11.**  
 The Cauer synthesis of the three-decade RC ladder model.

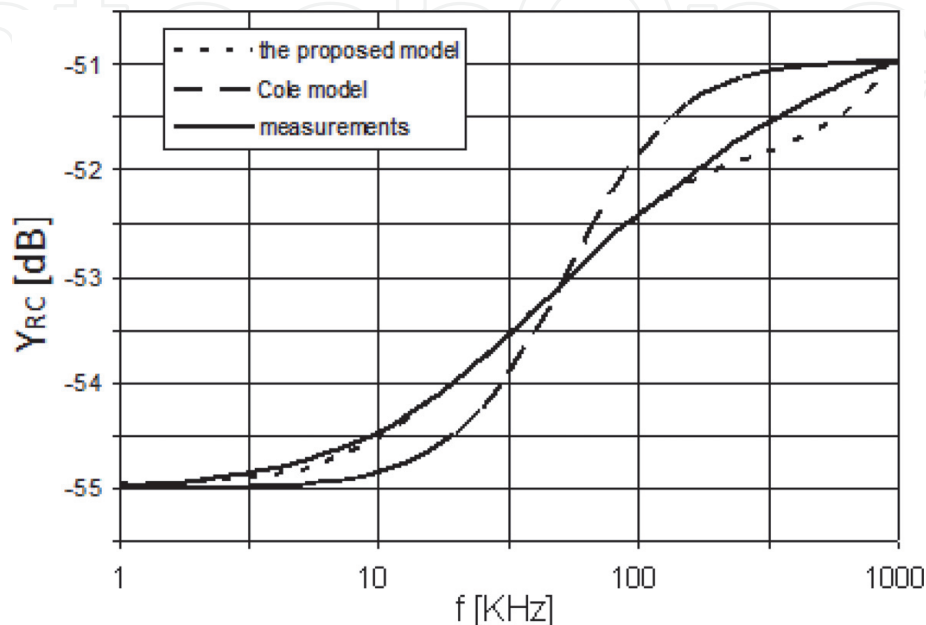


**Figure 12.**  
 The frequency characteristic of the Cole model, the three-decade RC ladder model and the measured results.

## 5. RC parallel model

### 5.1 Introduction

A behavioral model, as a linear circuit which can be an extension of the Cole model is the best choice, taking into account that the intracellular and the extracellular water volumes are related to the real part of the model impedance computed at minimum and maximum frequencies [3], this impedance being well defined only for a model of this kind.

An RC parallel model, valid for a frequency range of three decades, which can be reduced to the Cole model for a narrow frequency interval, is presented in this section.

### 5.2 Parameter identification for the RC parallel model

For the parameter identification of the RC parallel model, only the measured frequency characteristic  $|Y_{RC}(j\omega)|$  is used [10]. In order to build this model, the approximation method is employed, followed by the circuit synthesis as it is described in the previous section.

Using the above algorithm, the frequency characteristic  $|Y_{RC}(j\omega)|$  corresponding to the data in [3] has been approximated by the admittance in Eq. (6) with an error  $\varepsilon = 0.95$  dB using a sweeping step  $\Delta\omega_m = 8315$  Hz. The synthesis of this admittance can be made by the Foster II method which gives the most interesting circuit in **Figure 13**.

The direct employment of the Foster II synthesis algorithm starting from Eq. (6) leads to some negative parameter values. This effect can be avoided performing the Foster II synthesis of  $|Y_{LC}(j\omega)|$ , where  $Y_{LC}(s)$  in Eq. (9) is given by the frequency transformation in Eq. (8) [17].

$$Y_{LC}(s) = \frac{1}{s} \cdot Y_{RC}(s^2) \tag{8}$$

$$Y_{LC}(s) = 19.47 \cdot 10^{-11}s + \frac{17.81 \cdot 10^4}{s} + \frac{24.14 \cdot 10^{-10}s}{11.54 \cdot 10^{-6}s^2 + 1} + \frac{94.53 \cdot 10^{-11}s}{38.08 \cdot 10^{-7}s^2 + 1} + \frac{50.94 \cdot 10^{-11}s}{16.47 \cdot 10^{-7}s^2 + 1} + \frac{59.04 \cdot 10^{-13}s}{15.91 \cdot 10^{-5}s^2 + 1} \tag{9}$$

Starting from the partial fraction decomposition in Eq. (9), the parameter values are:  $C5 = 5.9$  pF,  $R5 = 27$  M $\Omega$ ,  $C4 = 2.41$  nF,  $R4 = 4.78$  k $\Omega$ ,  $C3 = 0.945$  nF,  $R3 = 4.03$  k $\Omega$ ,  $C2 = 0.51$  nF,  $R2 = 3.23$  k $\Omega$ ,  $C1 = 0.195$  nF,  $R1 = 561.5$   $\Omega$ .

The resistance corresponding to the volume of the extracellular water can be computed for  $f_{min} = 1$  kHz and has a 560.97  $\Omega$  value, which is practically the same with  $R_E = 562$   $\Omega$  given by the Cole model.

The resistance corresponding to the volume of the intracellular water can be computed for  $f_{max} = 1000$  kHz and has a 314.97  $\Omega$  value, unlike  $R_i = 352.69$   $\Omega$  given by the Cole model. Due to the better agreement with experimental data, it is expected that the body water volume prediction will be improved considering these values in Eqs. (1) and (2).

It is very interesting to observe that  $R1$  has a similar value to  $R_e$  in the Cole model, being the equivalent resistance for  $f = 0$  Hz. This circuit can be viewed as a generalization of the Cole model. The two branch models contain  $R1, R2, C2$ . As the frequency range of interest is extended to higher frequencies, a model with a greater number of branches is needed. The simulated data obtained with models with various numbers of branches, obtained by imposing the same error  $\epsilon$  on various frequency intervals are given in **Figure 14**.

A similar circuit (**Figure 15**) is given in [3] without pointing out how the resistance and capacitance values can be computed starting from the measured data.

In order to appreciate the agreement between the measured and simulated data, the measuring errors must be known. Unfortunately, no information on these errors is given in [3].

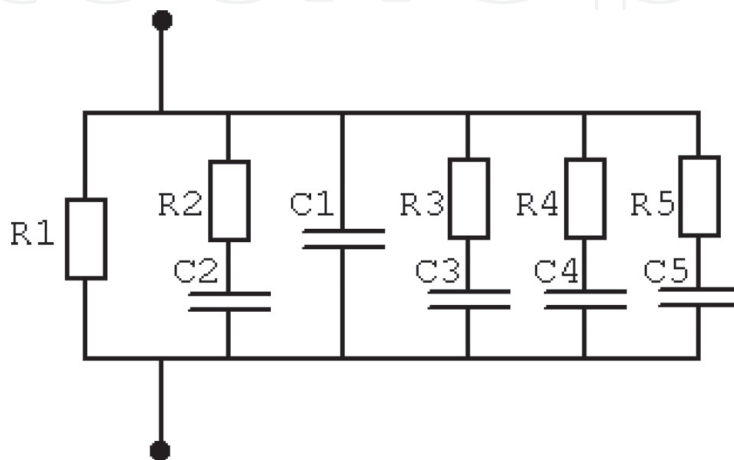


**Figure 13.** Foster II synthesis of the new circuit model [10].

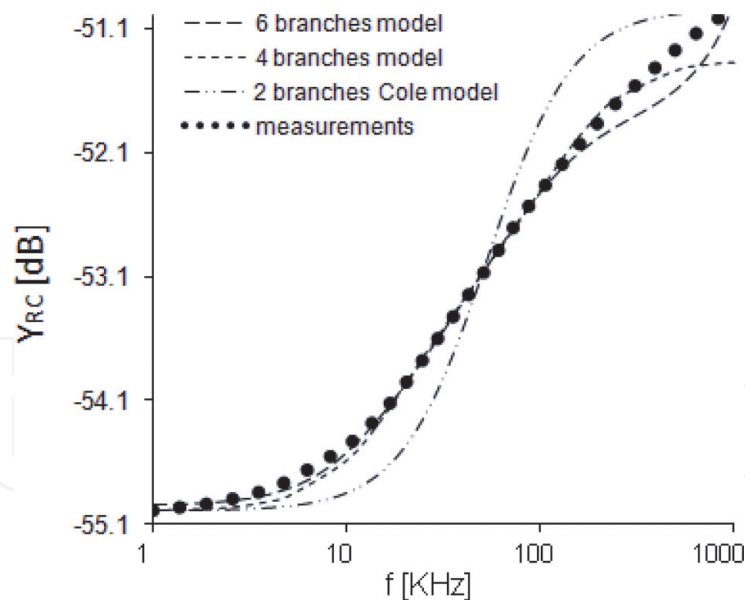


**Figure 14.**  
 The measured frequency characteristic and some proposed models with 2, 4 and 6 branches [10].

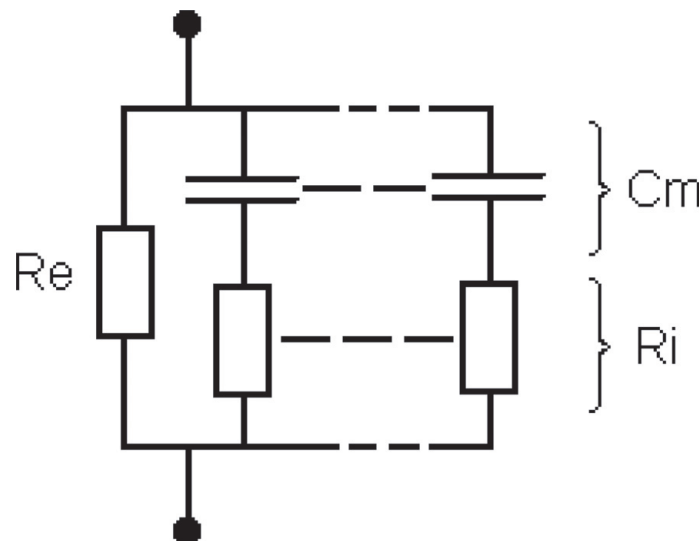


**Figure 15.**  
 The extended Cole model [3].

## 6. Conclusions

Four models of the human body bioimpedance used to compute ICW and ECW volumes have been presented in this chapter.

The first model presented in this chapter is the Cole model. This model is used for body water volume prediction, having frequency independent values for  $R_i$ ,  $R_e$  and  $C_m$ . It cannot reproduce the measurement results for a three or even for a two-decade frequency range.

The second model is based on a fractional exponent formula for the body impedance whose module is fitted to the measured values in [3]. But the real part of this impedance at the minimum and maximum frequencies cannot be computed and, consequently, the ICW and ECW formulae, having an outstanding practical importance, cannot be used.

The next two behavioral models are based on parameter identification. These models are linear RC circuits with frequency independent elements, whose

parameters can be identified starting from the measured values  $|Z_{RC}(j\omega)|$  reported in [3]. The influence of the measurement equipment including signal source, cables (modeled as transmission lines) and connectors has been shown to be negligible, so  $|Z_{RC}(j\omega)|$  given in [3] is an accurate representation of the human body impedance modulus [8, 18].

After the synthesis of the third model, an *RC* ladder, valid for a frequency range between 1 and 100 kHz [8], and its extension to a three-decade frequency interval [17], the fourth model, the *RC* parallel circuit [9], whose validity range is three decades is presented. This model contains some *RC* branches connected in parallel. This model can be simplified, taking into account that the influence of some branches is negligible in a certain frequency range, its ultimate simplification being the linear *RC* Cole model. It follows that this model can be considered as an extension of the linear *RC* Cole model, allowing a good prediction of the intracellular and extracellular water volumes. All these linear lumped *RC* circuits avoid using both intricate frequency dependent elements suggested by the physical interpretation of current conduction in human body and the fractional exponent impedance formula of de Lorenzo model [3].

Even though the modeling of fractional-order circuits is rigorously established [19], a linear *RC* circuit model based on straightforward concepts is more useful for intracellular and extracellular water volume prediction than a fractional-order system. The development of these new models illustrates the actual trend [20] to make noninvasive investigation methods more precise in various areas of medicine [7] as coronary artery disease [21], colorectal cancer [22] and HIV infection [23].

IntechOpen

### **Author details**

Alexandru Gabriel Gheorghe\*, Florin Constantinescu, Miruna Nițescu  
and Mihai Eugen Marin  
University Politehnica of Bucharest, Romania

\*Address all correspondence to: alexandru.gheorghe@upb.ro

### **IntechOpen**

© 2020 The Author(s). Licensee IntechOpen. This chapter is distributed under the terms of the Creative Commons Attribution License (<http://creativecommons.org/licenses/by/3.0>), which permits unrestricted use, distribution, and reproduction in any medium, provided the original work is properly cited. 

## References

- [1] Mattie J, Zarowitz B, De Lorenzo A, Andreoli A, Katzarski K, Pan G, et al. Analytic assessment of the various bioimpedance methods used to estimate body water. *Journal of Applied Physiology*. 1998;**84**:1801-1816
- [2] Lichtenbelt WDM, Westerterp KR, Wouters L, Luijendijk SCM. Validation of bioelectrical-impedance measurements as a method to estimate body-water compartments. *American Journal of Clinical Nutrition*. 1994;**60**: 159-166
- [3] De Lorenzo A, Andreoli A, Matthie J, Withers P. Predicting body cell mass with bioimpedance by using theoretical methods: A technological review. *Journal of Applied Physiology*. 1997; **82**(5):1542-1558
- [4] Gudivaka R, Schoeller DA, Kushner RF, Bolt MJG. Single- and multifrequency models for bioelectrical impedance analysis of body water compartments. *Journal of Applied Physiology*. 1999;**87**(3):1087-1096
- [5] Matthie JR. Second generation mixture theory equation for estimating intracellular water using bioimpedance spectroscopy. *Journal of Applied Physiology*. 2005;**99**(2):780-781
- [6] Earthman C, Traughber D, Dobratz J, Howell W. Bioimpedance spectroscopy for clinical assessment of fluid distribution and body cell mass. *Nutrition in Clinical Practice*. 2007; **22**(4):389-405
- [7] Marin CV. Frequency selection for parameter identification in bioimpedance spectroscopy. *Revue Roumaine Des Sciences Techniques*. 2009;**54**(4):425-434
- [8] Gheorghe AG, Marin CV, Constantinescu F, Nitescu M. Synthesis of a new RC model for body cell mass prediction. In: National Symposium on Theoretical Electrical Engineering, Politehnica University, June 5–7. 2008
- [9] Schwan HP. Electrical properties of tissues and cell suspensions: Mechanisms and models. In: Proceedings of 16th Annual International Conference of the IEEE Engineering in Medicine and Biology Society. 1994. pp. 70-71
- [10] Gheorghe AG, Marin CV, Constantinescu F, Nitescu M. Parameter identification for a new circuit model aimed to predict body water volume. *Advances in Electrical and Computer Engineering*. 2012;**12**(4):83-86
- [11] Constantinescu F, Marin CV, Nitescu M, Marin D. Parameter identification using symbolic pole/zero expressions. In: European Conference on Circuit Theory and Design (ECCTD'03), Poland, September 1–4. 2003
- [12] Avitabile G, Fedi G, Giomi R, Luchetta A, Manetti S, Piccirilli MC. Parameter extraction in electronic device modelling using symbolic techniques. In: Proceedings of the Second International Workshop on Symbolic Methods and Applications to Circuit Design, October 8–9. Germany: Kaiserslautern; 1998. pp. 253-261
- [13] Konkzykowska A, Rozes P, Bon M. Parameter extraction of semiconductor devices electrical models using symbolic approach. In: Proceedings of the Second International Workshop on Symbolic Methods and Applications to Circuit Design, October 8–9. Italia: Firenze; 1992. pp. 1-10
- [14] Burmen A, Tuma T. Model parameter identification with SPICE OPUS: A comparison of direct search and elitistic genetic algorithm. In: Proceedings of ECCTD'01. 2001. pp. 61-64

- [15] Bandler JW, Chen SH, Ye S, Zhang Q-J. Integrated model parameter extraction using large scale optimization concepts. *IEEE Transactions on Microwave Theory and Techniques*. 1988;**36**(12):1629-1638
- [16] Constantinescu F, Gheorghe AG, Ioan CD, Nitescu M, Iordache M, Dumitriu L. A new approach to the computation of reduced order models for one-port and two-port RC circuits. In: *International Symposium on Circuits and Systems (ISCAS)*, May 21–24. Greece: Island of Kos; 2006. pp. 4002-4005
- [17] Guillemin EA. *Synthesis of Passive Networks - Theory and Methods Appropriate to the Realization and Approximation Problems*. New York: John Wiley & Sons; 1967
- [18] Gheorghe AG, Marin CV, Constantinescu F, Nitescu M. A new circuit model for body cell mass prediction. In: *4th European Conference on Circuits and Systems for Communications (ECCSC 08)*, Jul 10–11. Romania: Politehnica University, Bucharest; 2008
- [19] Elwakil AS. Fractional order circuits and systems: An emerging interdisciplinary research area. *IEEE Circuits and Systems Magazine*. 2010; **10**(4):41-44
- [20] Zhurbenko V. Challenges in the design of microwave imaging systems for breast cancer detection. *Advances in Electrical and Computer Engineering*. 2011;**11**(1):91-96
- [21] Singh RB, Niaz MA, Beegom R, Wander GS, Thakur AS, Rissam HS. Body fat percent by bioelectrical impedance analysis and risk of coronary artery disease among urban men with low rates of obesity: The indian paradox. *Journal of the American College of Nutrition*. 1999;**18**(3):268-273
- [22] Gupta D, Lammersfeld CA, Burrows JL, Dahlk SL, Vashi PG, Grutsch JF, et al. Bioelectrical impedance phase angle in clinical practice: Implications for prognosis in advanced colorectal cancer. *The American Journal of Clinical Nutrition*. 2004;**80**:1634-1638
- [23] Earthman CP, Mattie JR, Reid PM, Harper IT, Ravussin E, Howell WH. A comparison of bioimpedance methods for detection of body cell mass change in HIV infection. *Journal of Applied Physiology*. 2000;**88**:944-956